

Mechanism of the Quenching of the Hall Effect

George Kirczenow

Department of Physics, Simon Fraser University, Burnaby, British Columbia, Canada V5A 1S6

(Received 8 February 1989)

Quantum mechanical calculations of electron scattering at junctions of 1D conductors are presented together with an analysis of the implications for experimentally measured transport coefficients. Resonant electron states intrinsic to such junctions give rise to quenching of the Hall voltage, maxima in the longitudinal resistance, and anomalous Hall plateaus. At high B they show up as sharp features in R_H and R_L which track the bottoms of 1D subbands. Quenching of the Hall voltage is found for ≤ 3 populated 1D subbands. The other resonant phenomena occur also at higher band fillings.

PACS numbers: 72.20.My, 73.20.Dx, 73.50.Jt

Simple considerations of electromagnetic theory suggest that the Hall effect should be a universal phenomenon common to all metallic systems. Thus the report by Roukes *et al.*¹ of the disappearance of the Hall voltage across a quasi-one-dimensional (1D) conductor at low magnetic fields came as a surprise and was met with some initial skepticism, although in retrospect it appears that certain anomalies in the data of Simmons, Tsui, and Weimann² and Timp *et al.*³ were precursors of this phenomenon. Clear confirmation of the quenching of the Hall voltage has now been reported by Timp *et al.*⁴ and Ford *et al.*,⁵ but the physical mechanism responsible has remained a mystery. Using the Büttiker formalism,⁶ Peeters⁷ and Akera and Ando⁸ calculated the Hall resistance of a 1D conductor for weakly coupled Hall probes, and found *no* quenching. Peeters⁷ suggested that the observed quenching may be due to strong coupling of the Hall probes to the 1D conductor in the experiments, and this idea has been supported by Kirczenow.⁹ In this article the physics of electron transport at quantum wire junctions is studied in some detail in the strongly coupled regime. It is shown that resonant states which are intrinsic to junctions of ultranarrow conductors should manifest themselves at low B in quenching of the Hall effect, anomalous plateaus in the Hall resistance R_H , and peaks in the longitudinal resistance R_L . Such resonant states have been predicted by Peeters,¹⁰ by Kirczenow⁹ and, at $B=0$, by Schult, Ravenhall, and Wyld,¹¹ but their implications for magnetotransport measurements were not fully understood. Low- B phenomena similar to those described above have been observed in quantum wires by various groups.^{1-5,12} However, in the present calculations the resonant quenching of the Hall voltage is found for somewhat narrower conductors than those which appear to have been studied to date experimentally. The other predicted resonant phenomena should occur in the currently available systems but will be more pronounced in narrower conductors. It is hoped that this work will stimulate the development of microstructures in which the interesting physics of resonant electron scattering predicted here will be easier to observe.

The system to be considered is shown in Fig. 1, inset (a). Four quantum wires connected to electron reservoirs at chemical potentials μ_α join at right angles. A magnetic field \mathbf{B} is oriented perpendicular to the plane of the cross. R_H and R_L for this system can be found from the Büttiker equations⁶

$$I_\alpha = \left(i\mu_\alpha - \sum_\beta T_{\alpha\beta} \mu_\beta \right) q_e / h, \quad (1)$$

where I_α is the current in the lead α , and $T_{\alpha\beta}$ is the probability that an electron in lead β is scattered into lead α . $T_{\alpha\alpha}$ are reflection coefficients. All leads are assumed identical and i is the number of populated channels (subbands plus spin) per lead. All spin splittings will be ignored. The $T_{\alpha\beta}$ were calculated assuming the potential confining electrons to the quantum wires to be parabolic, as is suggested by the theory of Laux, Frank, and Stern¹³ for the narrowest uniform quantum wires in semiconductor heterostructures. The model potential energy of the electrons in the x - y plane was chosen as

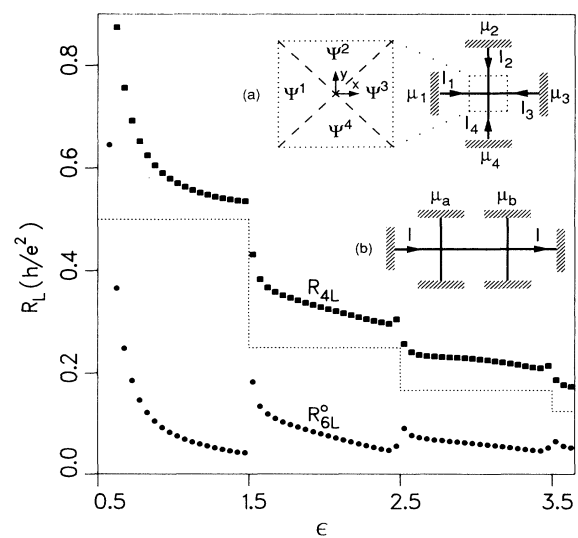


FIG. 1. R_L vs Fermi energy at $B=0$. Insets (a), (b): Four- and six-probe geometries.

$V(x,y)=cx^2$ for $|y| > |x|$ and $V(x,y)=cy^2$ for $|x| > |y|$ for quantum wires running along the x and y axes as in the inset. In the symmetric gauge $\mathbf{A}=(-By/2, Bx/2, 0)$. The one-electron Hamiltonian is $H=(\mathbf{p}-q_e\mathbf{A})^2/2m^*+V(x,y)$. In each of the four quantum wires (whose boundaries are dashed lines at $x=\pm y$ in Fig. 1), H has eigenfunctions belonging to 1D subband n ($=0, 1, 2, \dots$) given by

$$\begin{aligned}\psi_{nk}^\rho(x,y) &= e^{ix(k+Bq_e y/2\hbar)} u_{nk}^\rho(y), \\ \psi_{nk}^\sigma(x,y) &= e^{iy(k-Bq_e x/2\hbar)} u_{nk}^\sigma(x).\end{aligned}$$

Here ρ stands for wire 1 or 3 and σ for 2 or 4. The u_{nk}^ρ and u_{nk}^σ are displaced harmonic-oscillator eigenfunctions. For an electron in subband n having energy E and wave vector k , which is incident on the junction from wire 1, the electron eigenstate is given by $\Psi=\Psi^1, \Psi^2, \Psi^3$, and Ψ^4 in wires 1, 2, 3, and 4, respectively, where $\Psi^1(x,y)=\Psi_{nk}^1+\sum_r a_r^1 \psi_{r,-k}^1$ and $\Psi^\eta(x,y)=\sum_r a_r^\eta \psi_{r,\pm k}^\eta$ for $\eta=2, 3$, and 4. The $+$ is for $\eta=2$ and 3; the $-$ is for $\eta=4$. In the summations, k_r is the wave vector of a partial wave with energy E in subband r . The sums are over *all* subbands, including those with imaginary k_r (evanescent partial waves). The expansion coefficients a_r^η and hence the scattering probabilities $T_{\alpha\beta}$ were found numerically from the continuity of Ψ and $\nabla\Psi$ at $x=\pm y$.

In the four-lead Hall geometry¹⁴ [Fig. 1, inset (a)] R_H and R_L are found from the Büttiker equations setting $I_1=-I_3=I$ and $I_2=I_4=0$:

$$\begin{aligned}R_{4H} &\equiv (\mu_2 - \mu_4)/Iq_e = (h/q_e^2)(T_{21} - T_{41})/Z, \\ R_{4L} &\equiv (\mu_1 - \mu_3)/Iq_e = (h/q_e^2)(T_{21} + T_{41} + 2T_{31})/Z,\end{aligned}$$

where

$$Z = T_{21}^2 + T_{41}^2 + 2T_{31}(T_{31} + T_{21} + T_{41}).$$

In interpreting both numerical results and measurements, R_L is as important as R_H . Experimentally R_H is obtained from a four-lead measurement; however, a six-lead measurement is used for R_L as shown in Fig. 1, inset (b).¹² The measured quantity is $R_{6L}=(\mu_a - \mu_b)/Iq_e$ (for zero current in the Hall leads). There is a major physical difference between R_{6L} and R_{4L} which can be understood as follows: If it is assumed that (i) there is no phase coherence between the two junctions in inset (b), (ii) there is complete randomization of electrons between different subbands as they pass between the two junctions, and (iii) electron backscattering by impurities can be neglected, then the six-probe Büttiker equations yield the simple result that $R_{6L}=R_{\delta L}^0 \equiv R_{4L} - h/iq_e^2$, where i is the number of populated channels, as in (1). R_{4L} and $R_{\delta L}^0$ calculated at $B=0$ are shown in Fig. 1 as a function of the normalized Fermi energy $\epsilon = E_F/\hbar\omega_0$, where $\hbar\omega_0 = \hbar(2c/m^*)^{1/2}$ is the subband splitting at $B=0$. The dotted line is h/iq_e^2 . Qualitatively, R_{4L} looks like the quantized two-probe resistance of a ballistic quantum channel,¹⁵ modified by the influence of the

junction. By analogy with Imry,¹⁶ one can think of the difference h/iq_e^2 between R_{4L} and $R_{\delta L}^0$ as a "contact resistance" between the reservoirs and wires 1 and 3 in the four-probe case, which is eliminated in a six-probe measurement. Then $R_{\delta L}^0$ can be interpreted as the resistance due to electron scattering by the leads, which has recently been the subject of an interesting study by Timp *et al.*⁴ In this paper the importance of *resonant* scattering by the leads is demonstrated. In the quasiballistic samples studied experimentally, conditions (i) and (ii) are probably satisfied but (iii) is not, so that one should write $R_{6L}=R_{\delta L}^0+R_B$, where R_B is a phenomenological backscattering correction which can be evaluated by measurements.¹² R_B can be large at small B but decreases as B increases, and vanishes when B becomes so large that the sample is effectively two dimensional and in the quantum Hall regime, as has been discussed by Büttiker.¹⁷

In the present model R_{4H} , R_{4L} , and $R_{\delta L}^0$ depend on two variables, the normalized Fermi energy ϵ and the normalized cyclotron frequency $\omega = \omega_c/\omega_0$. The results when only the lowest subband contains electrons are shown in Fig. 2, where R_{4H} (solid), $R_{\delta L}^0$ (dashed), and R_{4L} (dashed, left scale) are plotted for different ϵ which increases from curve *a* to curve *f*. R_H is quenched at low B , except at low ϵ where it is linear in B for small B . The range of B in which R_H is quenched increases with increasing Fermi level. This qualitative trend is contrary to the earlier phenomenology of Beenakker and van Houten¹⁸ (BvH) and was unanticipated. Experiments in the one-band regime are needed to test the present prediction. One should note, however, that even in the multiple-band regime, the model of BvH disagrees qualitatively with the measurements of Roukes *et al.*¹² Except in case *a* (where the band is magnetically depopulated in the range shown), there is a quantum Hall plateau (QHP) at large ω where $R_H \rightarrow h/2q_e^2$. The local minima exhibited by R_H in curves *e* and *f* are highly

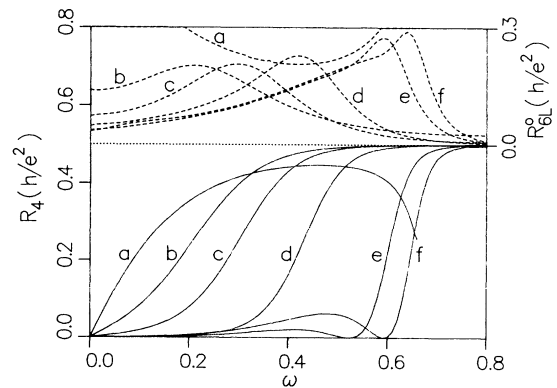


FIG. 2. R_{4H} (solid curves) and R_{4L} and $R_{\delta L}^0$ (dashed curves) vs ω for one occupied subband. Curves *a, b, c, d, e, and f* are for $\epsilon=0.6, 0.8, 1.0, 1.2, 1.4$, and 1.45 .

significant and will be discussed below. R_L exhibits a maximum, which is also important, in the ω range where R_H makes the transition from the QHP into the quench zone. Notice that at large magnetic fields $R_{4L} \rightarrow h/2q_e^2$, while $R_{\delta L}^0 \rightarrow 0$.

Some examples of R_H (solid curves) and $R_{\delta L}^0$ (dashed curves) vs ω for multiple occupied bands are shown in Fig. 3. At $B=0$, two subbands ($n=0$ and 1) are populated for $\epsilon=1.9$ and 2.4, and three for $\epsilon=3.4$. Vertical dotted lines mark where subband n empties. The accurate matching of $R_{\delta L}^0$ across these lines (where h/iq_e^2 changes) is quite remarkable. There is no quenching of R_H for $\epsilon=1.9$, quenching at $\epsilon=2.4$, and incipient quenching for $\epsilon=3.4$. The minima in R_H and maxima in R_L marked with the asterisks are due to resonant states localized at the junction. The existence of these states is expected theoretically.^{10,11} Physically they exist because an electron near the junction can lower its kinetic energy relative to that away from the junction by extending its wave function into all four arms of the cross. Such resonant states cause enhanced backscattering of electrons at the junction, and hence a peak in R_L . Recently Büttiker^{19,20} discussed the effect of junction impurity states on the $T_{\alpha\beta}$ and hence on four-probe resistance measurements. His argument applies also to intrinsic junction resonances and shows that they should depress R_H . The features in Fig. 3 that are the key to understanding the quenching of the Hall effect are marked by pointers. They are steps in R_H (some involving weak local minima) and associated broad maxima in R_L . Figure 4 shows the locations of the minima of R_H (full circles) and maxima of R_L (open circles) obtained from a series of scans like those in Fig. 3. They lie on trajectories running from high ϵ and ω to low ϵ and ω . At the high- ω end of each trajectory a sharp maximum of R_L coincides with a sharp minimum of R_H [the obvi-

ous resonances (asterisks) in Fig. 3], but towards the low- ω end, the minimum of R_H evolves continuously into a step, while the maximum in R_L broadens and weakens. We conclude that while the signature of a junction resonance at high magnetic fields is a sharp peak in R_L coincident with a minimum in R_H , at low fields it is a broad maximum in R_L and a step in R_H . The case $\epsilon=3.4$ in Fig. 3 shows five resonances (asterisks and pointers) at different stages of evolution from the high-field to the low-field form. A striking example is the evolution of the right-hand resonance (asterisk) at $\epsilon=1.9$ in Fig. 3 into the step in R_H and maximum of R_L which mark the edge of the quench zone in Fig. 2. Curves e and f in Fig. 2 show the last vestiges of the minimum in R_H before it disappears and the simple step down into the quench evolves. All of the quench zones in Fig. 4 are associated with resonances in this way, so that in this model the quenching is clearly the result of the steps in R_H which are low-field manifestations of junction resonances. Notice how the resonant maxima of R_L (open circles, Fig. 4) track the boundaries of the quench zones (dashed lines). Maxima of R_L at low B have often been observed experimentally in conjunction with quenching of R_H ,^{1,5,12} but there are some indications that this may have been fortuitous. The present theory predicts that

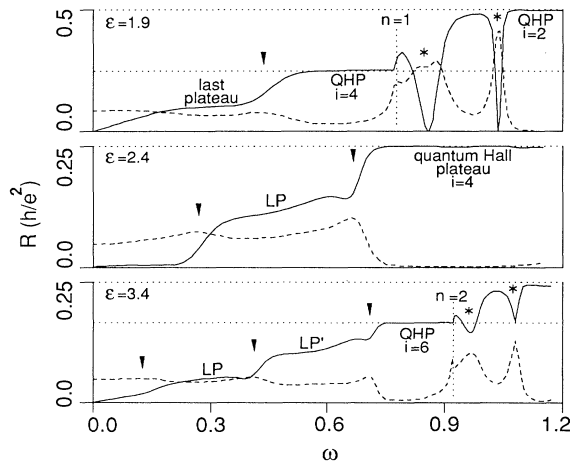


FIG. 3. R_{4H} (solid curves) and $R_{\delta L}^0$ (dashed curves) vs ω for multiple occupied bands.

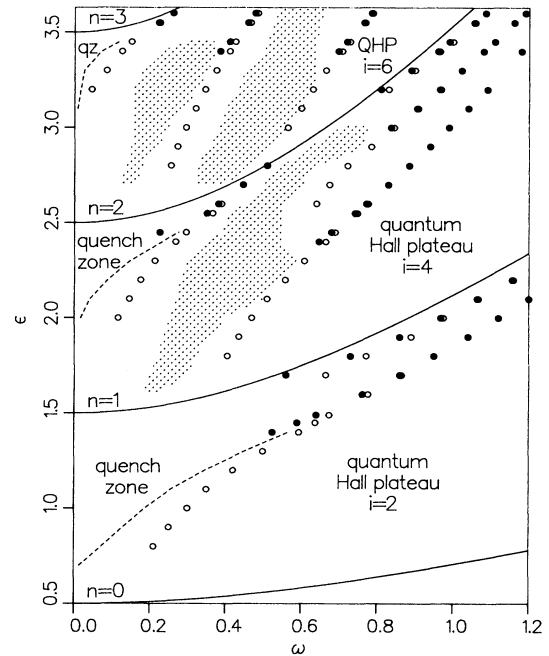


FIG. 4. Global map of predictions of the model. Solid curves are bottoms of subbands. Open (full) circles are maxima of R_L (minima of R_H) which locate the junction resonances. Shaded areas are "last plateaus." Boundaries of quench zones (dashed curves) are located by extrapolating to zero R_H the slope of R_H vs ω curves at their inflection points. Only incipient quenching occurs in the area labeled "qz."

the quenching of R_H should disappear and then reappear if the Fermi level is varied monotonically over a wide enough range at low B as is evident from Fig. 4. This effect is a direct consequence of the quenching being due to resonances. Qualitatively similar behavior has been observed by Roukes *et al.*,¹² but their samples have higher electron densities than those at which quenching is found in the present model. The present model predicts quenching when three or fewer subbands are occupied, although the other predicted resonant phenomena are not restricted to this range. The features in R_H labeled "last plateau," LP, and LP' in Fig. 3 (shaded areas in Fig. 4) clearly are also due to steps in R_H associated with junction resonances. Such plateaus are seen experimentally,^{1-5,12} and were at one time thought to be imperfect quantum Hall plateaus. The present calculations suggest that they are not. Unlike the LP's, the true quantum Hall plateaus found here do not slope and are accurately quantized according to $R_H = h/iq_e^2$. Notice that the LP's in Fig. 3 do *not* correspond to R_H near h/iq_e^2 for integer i .

Other interesting physics of the resonances may also be inferred from Fig. 4: The bottoms of the 1D subbands (BSB's) are shown as solid curves. At high ω , the energies of resonances just below a BSB *accurately* track that BSB. This suggests that it may be useful to think of these resonances as bound states of the subband just above them. They are, of course, unbound relative to lower subbands. This simple picture explains why the resonances closest to the $n=1$ and 2 BSB's disappear abruptly when they pass above the solid curves in Fig. 4—they become unbound relative to the subband to which they primarily belong. It also explains the broadening of the resonances at lower ω (where their energy is lower): The lower energy implies a larger admixture of lower subbands to the state and hence a shorter resonance lifetime.

In conclusion, resonant scattering at quantum wire junctions has been predicted to result in a richness of remarkable physical phenomena. Its presence at low B suggests that it may have practical implications for microcircuit design.

I thank M. L. Roukes for many illuminating conversations, and for sharing with me the novel experimental results, and E. Castaño, D. Boal, R. Barrie, and K. Visvanatan for their comments. The hospitality of Bellcore during a very productive visit is greatly appreciated. This work was supported by the Natural Sciences and Engineering Research Council of Canada.

Note added.—Since this work was submitted for publication I have become aware of independent work by Ravenhall, Wyld, and Schult,²¹ who use a square-well confining potential to study electron scattering at junctions, and by Baranger and Stone,²² who argue that the quenching of the Hall voltage is due to collimation of electrons in tapered junctions. Collimation effects may

be relevant to some of the earlier data^{1,4,5} and to recent results of Chang and Chang²³ and of Timp,²⁴ but do not explain the measurements of Roukes *et al.*¹² Ford *et al.*²⁵ have recently demonstrated experimentally another geometry-dependent quenching mechanism based on electron reflections from surfaces within junctions.

¹M. L. Roukes, A. Scherer, S. J. Allen, Jr., H. G. Craighead, R. M. Ruthen, E. D. Beebe, and J. P. Harbison, *Phys. Rev. Lett.* **59**, 3011 (1988).

²J. A. Simmons, D. C. Tsui, and G. Weimann, *Surf. Sci.* **196**, 81 (1988).

³G. Timp, A. M. Chang, P. M. Mankiewich, R. Behringer, J. E. Cunningham, T. Y. Chang, and R. E. Howard, *Phys. Rev. Lett.* **59**, 732 (1987).

⁴G. Timp, H. U. Baranger, P. deVegvar, J. E. Cunningham, R. E. Howard, R. Behringer, and P. M. Mankiewich, *Phys. Rev. Lett.* **60**, 2081 (1988).

⁵C. J. B. Ford, T. J. Thornton, R. Newbury, M. Pepper, H. Ahmed, D. C. Peacock, D. A. Ritchie, J. E. F. Frost, and G. A. C. Jones, *Phys. Rev. B* **38**, 8518 (1988).

⁶M. Büttiker, *Phys. Rev. Lett.* **57**, 1761 (1986).

⁷F. M. Peeters, *Phys. Rev. Lett.* **61**, 589 (1988).

⁸H. Aker and T. Ando, *Phys. Rev. B* **39**, 5508 (1989).

⁹G. Kirzenow, *Phys. Rev. Lett.* **62**, 1920 (1989).

¹⁰F. M. Peeters, in *Proceedings of the Fourth International Conference on Superlattices, Microstructures and Microdevices*, Trieste, Italy, 1988 (to be published).

¹¹R. L. Schult, D. G. Ravenhall, and H. W. Wyld, *Phys. Rev. B* **39**, 5476 (1989).

¹²M. L. Roukes, T. J. Thornton, A. Scherer, B. P. Van der Gaag, and E. D. Beebe (to be published).

¹³S. E. Laux, D. J. Frank, and F. Stern, *Surf. Sci.* **196**, 101 (1988).

¹⁴Using Büttiker's notation $R_{4H} = R_{1,3,2,4}$; $R_{4L} = R_{1,3,1,3}$.

¹⁵B. J. van Wees *et al.*, *Phys. Rev. Lett.* **60**, 848 (1988); D. A. Wharam *et al.*, *J. Phys. C* **21**, L209 (1988); G. Kirzenow, *Solid State Commun.* **68**, 715 (1988); *J. Phys. Condens. Matter.* **1**, 305 (1989); *Phys. Rev. B* **39**, 10452 (1989); A. Szafer and A. D. Stone, *Phys. Rev. Lett.* **62**, 300 (1989); E. G. Haanappel and D. van der Marel, *Phys. Rev.* **39**, 5484 (1989).

¹⁶Y. Imry, in *Directions in Condensed Matter Physics*, edited by G. Grinstein and G. Masenko (World Scientific, Singapore, 1986), Vol. 1.

¹⁷M. Büttiker, *Phys. Rev. B* **38**, 9375 (1988).

¹⁸C. W. J. Beenakker and H. van Houten, *Phys. Rev. Lett.* **60**, 2406 (1988).

¹⁹M. Büttiker, *Phys. Rev. Lett.* **62**, 229 (1989).

²⁰M. Büttiker, *Phys. Rev. B* **38**, 12724 (1988).

²¹D. G. Ravenhall, H. W. Wyld, and R. L. Schult, *Phys. Rev. Lett.* **62**, 1780 (1989).

²²H. U. Baranger and A. D. Stone (to be published).

²³A. M. Chang and T. Y. Chang (to be published).

²⁴G. L. Timp, in *Proceedings of the International Symposium on Nanostructure Physics and Fabrication*, College Station, TX, March 1989 (unpublished).

²⁵C. J. B. Ford *et al.*, *Phys. Rev. Lett.* **62**, 2724 (1989).